^{93}Nb NMR of the random-field-dominated relaxor transition in pure and doped SBN

R. Blinc, A. Gregorovič, B. Zalar, R. Pirc, and J. Seliger
Jožef Stefan Institute, P.O. Box 3000, 1001 Ljubljana, Slovenia

W. Kleemann
Laboratorium für Angewandte Physik, Gerhard-Mercator-Universität, 47048 Duisburg, Germany

S. G. Lushnikov
A. F. Ioffe Physical Technical Institute, 194021 St. Petersburg, Russia

R. Pankrath
Fachbereich Physik, Universität Osnabrück, Barbarastr. 7, 49069 Osnabrück, Germany

(Received 26 February 2001; published 13 September 2001)

The ferroelectric relaxor transitions in $Sr_{0.61}Ba_{0.39}Nb_2O_6$ (SBN61) and $Sr_{0.61-y}Ce_yBa_{0.39}Nb_2O_6$ (SBN61:Ce $y=0.0066$) have been studied by quadrupole perturbed ^{93}Nb NMR. The spectra are inhomogeneous frequency distributions $f(\nu)$ consisting of a central component due to the $1/2 \leftrightarrow -1/2$ transition and a broad background due to the satellite transitions. From the temperature dependence of the width and position of the central component spectrum and from the T dependence of T_2 we determined the T dependence of the Edwards-Anderson order parameter and of the normalized spontaneous polarization P. The random bond–random field Ising model parameters are $J_0=485$ K, $J=388$ K, and $\Delta/J^2=0.14$. The random-field contribution $\tilde{\Delta}=\Delta/J^2$ is here by two orders of magnitude larger than in the perovskite relaxor $PbMg_{1/3}Nb_{2/3}O_3$ (PMN).

DOI: 10.1103/PhysRevB.64.134109 PACS number(s): 61.43.−j, 77.84.Dy, 76.60.−k

I. INTRODUCTION

Strontium barium niobate,[1] $Sr_xBa_{1-x}Nb_2O_6$ (abbreviated as SBN), is a prototypical relaxor system[2,3] which belongs to the tetragonal tungsten bronze ferroelectric oxide family, AB_2O_6, rather than to the ABO_3 cubic perovskite family related to $PbMg_{1/3}Nb_{2/3}O_3$ (PMN). The congruently melting $Sr_{0.61}Ba_{0.39}Nb_2O_6$ (SBN61) is tetragonal both above $(4/mmm)$ and below $(4mm)$ $T_c=350$ K and shows below T_c a spontaneous polarization P along the tetragonal c axis.[4] The ferroelectric unit cell contains five AB_2O_6 units. Below T_c all metallic ions are shifted along the tetragonal polar axis. Above T_c the Ba^{2+} and Sr^{2+}, as well as 20% of the Nb^{5+} ions move towards symmetrical positions in the oxygen layers, whereas the residual 80% of the Nb^{5+} ions are equivalently distributed above and below the oxygen planes. The Ce^{3+} ions are known to substitute the Sr^{2+} ions. The system can be represented by the structural formula $A'_2A''_4C_4B'_2B''_8O_{30}$. The A' sites are occupied only by the Sr^{2+}, whereas the A'' sites are disordered and can be occupied both by the small Sr^{2+} and the larger Ba^{2+} ions. Only 5/6 of the A sites are occupied so that 1/6 of the A sites form vacancies. SBN61 is therefore referred to as an unfilled bronze.[4]

SBN type systems show in analogy to cubic relaxors giant polydispersivity and a huge sensitivity to external electric fields.[5] In spite of the random distribution of the Sr^{2+} and Ba^{2+} ions no macroscopic concentration gradients do occur as shown by microanalysis measurement so that wide distributions of the Curie temperatures as suggested earlier[2] cannot explain the relaxor properties. The primary source of the observed relaxor behavior is now believed[6–8] to be due to charge disorder induced polar nanoclusters which are dynamic entities above T_c but become frozen out and connected below T_c in the ferroelectric phase.

In PMN type cubic relaxors the order parameter field is quasicontinuous.[6] The interactions between the polar nanoclusters and the observed linear and nonlinear dielectric relaxor properties have been described with the spherical random bond–random field (SRBRF) model.[6,9] NMR investigations of PMN[6,7] and related crystals[10,11] have revealed both the dynamic character of the polar nanoclusters, as well as the temperature dependence of the Edwards-Anderson glass order parameter and the SRBRF predicted Gaussian line shape[6] which is very different from the ones seen in Ising type dipolar glasses[12] or simple inhomogeneous ferroelectrics. The proper description of uniaxial SBN type relaxor systems is still open and is at present the object of intensive research. Critical exponents emerging from the polarization autocorrelation function recently[4,13] suggested that SBN might be referred to as a random field dominated relaxor ferroelectric.

No NMR investigations of SBN type systems have been performed so far to the best of our knowledge. Here we report on an ^{93}Nb($I=9/2$) quadrupole perturbed NMR study of pure SBN61 and Ce^{3+} doped SBN61 (SBN61:Ce) single crystals. SBN61:Ce is known to exhibit enhanced relaxor properties.[14] We particularly wished to check on the microscopic nature of the polar nanoclusters and the relative magnitudes of the random field and random bond contributions. We also wanted to compare the obtained results with the ones previously found in perovskite type relaxors and see if the SRBRF model or the random bond–random field Ising model are applicable in the case of SBN.

II. EXPERIMENT

SBN61 and SBN61:Ce crystals with optical quality were grown by the Czochralski technique. Parallelepiped-shaped samples with {001} faces and size $V \approx 6\times4\times4$ mm^3 (long edge parallel to the polar c axis) were used in the NMR experiments. ^{93}Nb($I=9/2$) spin echo Fourier transform NMR spectra have been measured in a 9.2 T wide bore superconducting magnet at a ^{93}Nb Larmor frequency $\nu_L = \omega_L/2\pi = 92.92$ MHz. The width of the 90° pulse was 2.1 μs. The central $1/2 \leftrightarrow -1/2$ transition spectrum was studied via a Fourier transform of the spin echo, whereas the satellite $1/2 \leftrightarrow 3/2$, $3/2 \leftrightarrow 5/2$, $5/2 \leftrightarrow 7/2$, and $7/2 \leftrightarrow 9/2$ transition spectra were recorded by sweeping the irradiation frequency and measuring the spin echo intensity. The temperature dependence of ^{93}Nb spin-lattice relaxation rate T_1^{-1} was measured with the saturation pulse sequence: $90^\circ_x \ldots 90^\circ_x \ldots 90^\circ_x \ldots \tau - 90^\circ_y - 180^\circ$. The spin-spin relaxation rate T_2^{-1} has been measured with the Hahn $90^\circ_x - \tau - 90^\circ_y - \tau - echo$ sequence.

III. THEORY

A. Spin-spin and spin-lattice relaxation

The spin Hamiltonian of our problem is the sum of a large Zeeman term $\mathcal{H}_Z$, a time independent quadrupolar term $\mathcal{H}_Q$, a chemical shift term $\mathcal{H}_\sigma$, and a dipolar term $\mathcal{H}_D$, as well as a time dependent quadrupolar perturbation $\delta\mathcal{H}_Q(t)$:

$$\mathcal{H} = \mathcal{H}_Z + \mathcal{H}_Q + \mathcal{H}_\sigma + \mathcal{H}_D + \delta\mathcal{H}_Q(t) = \mathcal{H}_0 + \delta\mathcal{H}_Q(t). \quad (1)$$

The time dependent parts of $\mathcal{H}_\sigma$ and $\mathcal{H}_D$ are here neglected as they are small as compared to $\mathcal{H}_Q(t)$. If the z axis is chosen as the spin quantization axis, $\delta\mathcal{H}_Q(t)$ can be expressed as[15]

$$\delta\mathcal{H}_Q(t) = \left(\frac{eQ}{I(2I-1)}\right)[\delta V_0(t)(3I_z^2 - I(I+1)) + \delta V_{-1}(t) \times (I_+ I_z + I_z I_+) + \delta V_{+1}(t)(I_- I_z + I_z I_-) + \delta V_{-2}(t) I_+^2 + \delta V_{+2}(t) I_-^2], \quad (2)$$

where $V_0 = V_{zz}$, $V_{\pm1} = V_{xz} \pm iV_{yz}$, and $V_{\pm2} = (V_{xx} - V_{yy})/2 \pm iV_{xy}$ are combinations of coefficients V_{ij} of the electric field gradient (EFG) tensor in a coordinate frame with the z axis along the direction of the external magnetic field. In first order perturbation theory the eigenstates $|I,m\rangle$ of I_z are also eigenstates of the large Zeeman term $\mathcal{H}_Z$ and the small quadrupole term $\mathcal{H}_Q$. The density matrix $\rho(t)$ evolves in time according to the equation of motion

$$i\hbar \frac{d\rho(t)}{dt} = [\mathcal{H}_0 + \delta\mathcal{H}_Q(t), \rho(t)]. \quad (3)$$

The equation of motion can be most easily solved in the interaction picture. Omitting details which will be described elsewhere, we obtain the spin-spin relaxation rate from the time development of the off-diagonal elements of the transformed density matrix σ. For each off-diagonal element $|m,m+1\rangle$ we find a monoexponential time decay:

$$\frac{d\langle\sigma\rangle_{m,m+1}}{dt} = -W^{(2)}_{m,m+1}\langle\sigma\rangle_{m,m+1}, \quad (4)$$

where the average transition probability per unit time is given by

$$W^{(2)}_{m,m+1} = T_2^{-1} = C_0\left|\frac{eQ}{h}\right|^2 J(0) + C_1\left|\frac{eQ}{h}\right|^2 J(\omega_L) + C_2\left|\frac{eQ}{h}\right|^2 J(2\omega_L). \quad (5)$$

Here $J(0)$, $J(\omega_L)$, and $J(2\omega_L)$ represent the spectral densities of the autocorrelation functions of the EFG tensor elements δV_0, $\delta V_{\pm1}$, and $\delta V_{\pm2}$—which are related to the autocorrelation function of the order parameter field—at zero frequency, at the Larmor frequency ω_L, and at $2\omega_L$, respectively. The coefficients C_0, C_1, and C_2 are

$$C_0 = \frac{9\pi^2}{4[I(2I-1)]^2}(2m+1)^2, \quad (6a)$$

$$C_1 = \frac{\pi^2}{2[I(2I-1)]^2}[I(I+1)(8m^2+8m+6) - (8m^4+16m^3 + 34m^2+26m+9)], \quad (6b)$$

$$C_2 = \frac{\pi^2}{2[I(2I-1)]^2}[2I^2(I+1)^2 - 2I(I+1)(2m^2+2m+3) + (2m^4+4m^3+16m^2+14m+6)]. \quad (6c)$$

It should be noted that in view of the $(2m+1)^2$ factor $C_0 = 0$ for $m = -1/2$. For half-integer spin nuclei the central $1/2 \leftrightarrow -1/2$ transition T_2^{-1} thus does not reflect the low frequency EFG fluctuation spectra $J(0)$. For $I=9/2$ and the central $1/2 \leftrightarrow -1/2$ transition we thus have $C_0 = 0$, $C_1 = 0.37$, and $C_2 = 4.2$. For the $3/2 \leftrightarrow 1/2$ satellite transition, on the other hand, we have here $C_0 = 0.7$, $C_1 = 1.01$, and $C_2 = 3.88$. The above trend in the increase of C_0 and C_1 and decrease in C_2 continues (see Appendix A) until we find for the $9/2 \leftrightarrow 7/2$ satellite transition $C_0 = 1.1$, $C_1 = 3.29$, and $C_2 = 0.92$. The difference between the satellite and central transition T_2^{-1} can be thus used to estimate the low frequency fluctuation spectrum $J(0)$.

For the case of relaxors (or more generally, a glass) we have to take into account that the state of the system is in the fast motion limit characterized by a local polarization distribution function $W(p)$ and that T_2 itself will depend on the local polarization $T_2 = T_2(p) \propto (1-p^2)^{-3/2}$ (see Appendix B).

The T_2 decay of the magnetization can be written as

$$M_\perp(t) = \int_{-1}^{+1} W(p)\exp\left(-\frac{t}{T_2(p)}\right)dp. \quad (7)$$

For a relatively narrow local polarization distribution function $W(p)$ expression (7) can be approximated by an exponential decay: $M_\perp(t) \approx \exp(-t/T_{2\text{eff}})$.

The situation is somewhat different in the case of spin-lattice relaxation. Here EFG fluctuations induce transitions between the diagonal elements of $\langle\sigma\rangle$

$$\frac{d\langle\sigma\rangle_{m,m}}{dt}=\sum_k -W^{(1)}_{m,k}(\langle\sigma\rangle_{m,m}-\langle\sigma\rangle_{k,k}). \tag{8}$$

The average transition probabilities between the energy levels m and k per unit time $W^{(1)}_{m,k}$ correspond to the $\Delta m=\pm 1$ and $\Delta m=\pm 2$ transitions and are obtained as

$$W^{(1)}_{m,m+1}=\frac{\pi^2 J(\omega_L)}{2[I(2I-1)]^2}\left|\frac{eQ}{h}\right|^2(2m+1)^2[I(I+1)-m(m+1)], \tag{9a}$$

$$W^{(1)}_{m,m+2}=\frac{\pi^2 J(2\omega_L)}{2[I(2I-1)]^2}\left|\frac{eQ}{h}\right|^2[I(I+1)-m(m+1)]\times[I(I+1)-(m+1)(m+2)]. \tag{9b}$$

Neither the satellite nor the central transition spin-lattice relaxation rates here reflect the spectral density of fluctuations at zero frequency given by $J(0)$.

B. The spherical random bond–random field model

The uniaxial spherical random bond-random field (SRBRF) model Hamiltonian of a system of interacting polar nanoclusters can be written as[9]

$$\mathcal{H}=-\sum_{i,j} J_{ij}S_iS_j-\sum_i h_iS_i, \tag{10}$$

where the J_{ij} are infinitely ranged random interactions and h_i are quenched random fields assumed to obey independent Gaussian distributions characterized by their variances $[J^2_{ij}]^c_{\rm av}=J^2/N$ and $[h_ih_j]^c_{\rm av}=\delta_{ij}\Delta$ and mean values $[J_{ij}]^c_{\rm av}=J_0/N$ and $[h_i]^c_{\rm av}=0$. The brackets here designate the disorder average. For $J_0^2<J^2+\Delta$ the system forms a glass without long range order whereas for $J_0^2>J^2+\Delta$ a long range ordered inhomogeneous ferroelectric occurs below the transition temperature $T_c\approx J_0/k$.

The dimensionless order parameter field S_i is proportional to the cluster polarization. It is in fact a discrete quantity restricted to a large but finite number of values. In the simplest case we may assume that S_i fluctuates continuously

$$-\infty<S_i<\infty, \tag{11}$$

subject to the closure relation

$$\sum_i S_i^2=N, \tag{12}$$

where N denotes the total number of reorientable polar clusters. The local polarization of a cluster is defined in the fast motion limit as $p_i=\langle S_i\rangle$. The local polarization distribution function $W(p)=(1/N)\Sigma_i\delta(p-p_i)$ can be for $J>J_0$ expressed as

$$W(p)=\frac{1}{\sqrt{2\pi q}}\exp\left(-\frac{p^2}{2q}\right), \tag{13}$$

where q is the spherical glass Edwards-Anderson order parameter. $W(p)$ is thus here Gaussian at all temperatures. The glass order parameter q

$$q=\lim_{t\to\infty}\lim_{N\to\infty}\langle\langle S_i(0)S_i(t)\rangle_{t'}\rangle_{\rm dis}=\frac{1}{N}\sum_i\langle S_i\rangle^2 \tag{14}$$

is here for $J_0\to 0$ determined from the equation

$$q=\beta^2(1-q)^2(J^2q+\Delta), \tag{15}$$

where $\beta=1/kT$. For $J_0^2>J^2+\Delta$ and $T<T_c$ long range ferroelectric order appears and one has

$$W(p)=\frac{1}{\sqrt{2\pi(q-P^2)}}\exp\left[-\frac{1}{2}\frac{(p-P)^2}{q-P^2}\right], \tag{16a}$$

where P is the long range order parameter, i.e., the dimensionless normalized spontaneous polarization. P^2 is here given by

$$P^2=\left[1-\left(\frac{J}{J_0}\right)^2\right]\left(1-\frac{T}{J_0}\right)-\frac{\Delta}{J_0^2},\quad T<T_c \tag{16b}$$

and q by

$$q=1-\frac{T}{J_0}. \tag{16c}$$

The quadrupole perturbed NMR resonance frequency is for $T>T_c$ related to the local polarization p as

$$\nu=\nu_0+\nu_1p+\nu_2p^2+\cdots \tag{17}$$

resulting in an inhomogeneous NMR line shape $f(\nu)$

$$f(\nu)=\int W(p)\,\delta(\nu-\nu_0-\nu_1p-\nu_2p^2)dp \tag{18}$$

which is Gaussian for $|\nu_1|\gg|\nu_2|$ (linear case). The second moment of $f(\nu)$ is in the linear case proportional to the glass order parameter

$$M_2=\nu_1^2q. \tag{19}$$

If a quadratic term is present in the expansion (17) in addition to a linear one and $W(p)$ is symmetric, it is the first moment of $f(\nu)$ which is proportional to q

$$M_1=\nu_2q. \tag{20}$$

It should be noted that expression (20) is valid also in the ferroelectric case, where the presence of domains makes $W(p)$ symmetric. It is however not valid in a poled crystal where $W(p)$ is asymmetric. In this last case M_1 is given by

$$M_1=\nu_1P+\nu_2q. \tag{21}$$

C. The random bond–random field Ising model

In the random bond–random field (RBRF) Ising model the reorientable dipole can be described by an Ising pseudospin $S^z=\pm 1$ and the random bond–random field Hamiltonian is[16]

$$\mathcal{H}=-\sum_{i,j} J_{ij}S_i^zS_j^z-\sum_i h_iS_i^z, \tag{22}$$

where the infinitely ranged quenched random interactions J_{ij} and the quenched random fields h_i are introduced in analogy to the SRBRF model of Sec. III B. The local polarization distribution function $W(p)$ is however more complicated here:[12]

$$W(p)=\frac{1}{\beta\sqrt{2\pi(J^2q+\Delta)}}\frac{1}{1-p^2}\times\exp\left[-\frac{(\arctanh p-\beta J_0P)^2}{2\beta^2(J^2q+\Delta)}\right]. \tag{23}$$

In the glassy phase, which occurs for $J>J_0$, it is single peaked above $T_G\approx J/k$ and becomes double peaked well below T_G. The inhomogeneous NMR line shape $f(\nu)$ is obtained from $W(p)$ as

$$f(\nu)=\int_{-1}^{+1}W(p)\,\delta[\nu-\nu(p)]dp \tag{24a}$$

or equivalently

$$f(\nu)=\frac{W(p)}{\left|\frac{d\nu}{dp}\right|} \tag{24b}$$

with the help of the relation (17).

Here we again assumed to be in the fast motion regime where the NMR nucleus ''sees'' the time averaged value of the pseudospin $S_i^z(t)$, so that the local polarization is given by $p_i=\langle S_i^z\rangle$. The glass order parameter can be obtained from the moments of $f(\nu)$ in the same manner as described in Sec. III B. A ferroelectric transition occurs at $T_c\approx J_0/k$ provided that $J_0>J$. It should be noted that in the absence of random fields, i.e., for $\Delta=0$ and $J_0<J$, one has

$$q=0, \quad T>T_G=J/k, \tag{25a}$$

$$q>0, \quad T<T_G. \tag{25b}$$

For $J_0>J$ the glass order parameter q and the normalized polarization P are obtained from the following two coupled self-consistent equations:

$$q=\frac{1}{\sqrt{2\pi}}\int_{-\infty}^{\infty}e^{-x^2/2}\tanh^2(\beta\sqrt{J^2q+\Delta}\,x+\beta J_0P)dx, \tag{26a}$$

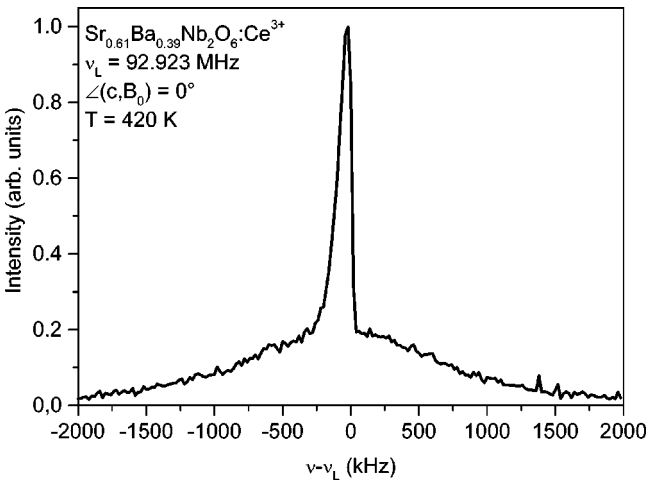

FIG. 1. The ^{93}Nb NMR line shape in SBN61:Ce at $T=420$ K for $\vec{c}\|\vec{B}_0$ and $\vec{a}\perp\vec{B}_0$ exhibiting a central $1/2\leftrightarrow-1/2$ component superimposed on a broad background due to satellite transitions. The slight asymmetry of the central component shows that in addition to the linear a small but nonzero quadratic term is also present in the expansion of the frequency in terms of the local polarization.

$$P=\frac{1}{\sqrt{2\pi}}\int_{-\infty}^{\infty}e^{-x^2/2}\tanh(\beta\sqrt{J^2q+\Delta}\,x+\beta J_0P)dx. \tag{26b}$$

It should be noted that according to Eqs. (26) the slope of the q vs T plot changes discontinuously at the the ferroelectric transition T_c. The change in the slope my be however hard to notice in the case of large random fields.

According to the x-ray[4] data the Nb^{5+} ions move in a double potential well which becomes asymmetric below T_c. For such a case one finds for the quadrupole perturbed satellite transitions

$$T_2^{-1}\approx C(1-p^2)^{3/2}. \tag{27}$$

IV. RESULTS

The ^{93}Nb quadrupole perturbed NMR spectrum of a SBN61:Ce single crystal is shown in Fig. 1 for $T=420$ K $>T_c$, $\vec{c}\|\vec{B}_0$, and $\vec{a}\perp\vec{B}_0$. Instead of sharp lines as in ordered crystals one finds here a frequency distribution consisting of a central component superimposed on a broad background. The spectra in SBN61 and SBN61:Ce are much broader than the corresponding ones found in cubic relaxors like PMN.[6] Both the central component, which is about 60 kHz broad, and the background, which extends over more than 4 MHz, are characteristic for ^{93}Nb spectra in charge and site disordered relaxors. What one expects to see is a central $1/2\leftrightarrow-1/2$ NMR transition shifted in second order by quadrupole interaction and four pairs of first order quadrupole split satellites corresponding to $\Delta m=\pm 1$ transitions $\pm 1/2\leftrightarrow\pm 3/2$, $\pm 3/2\leftrightarrow\pm 5/2$, $\pm 5/2\leftrightarrow\pm 7/2$, and $\pm 7/2\leftrightarrow\pm 9/2$. The relative intensities of these transitions are given by the matrix element $|\langle m|I_x|m-1\rangle|^2$ and amount to 9:16:21:24:25:24:21:16:9. The intensity of the central transi-

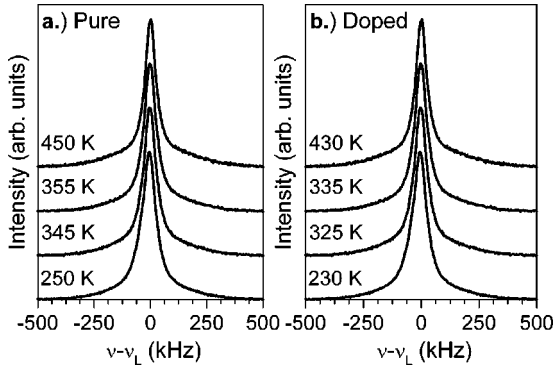

FIG. 2. Temperature dependence of the ^{93}Nb $1/2 \leftrightarrow -1/2$ NMR line shape in (a) SBN61 at the orientation $\theta = \angle(\vec{c}, \vec{B}_0) = 25°$: $T = 450$ K (100 K above $T_c = 350$ K), $T = 355$ K, $T = 345$ K, and $T = 250$ K; (b) SBN61:Ce at the orientation $\theta = \angle(\vec{c}, \vec{B}_0) = 25°$: $T = 430$ K (100 K above $T_c = 328$ K), $T = 335$ K, $T = 325$ K, and $T = 230$ K.

tion should thus amount to about 14% of the total NMR intensity. This indeed corresponds to the observed relative intensities of the central component and the broad background. One can thus ascribe the central component spectrum to a set of disorder induced shifts of the $1/2 \leftrightarrow -1/2$ transitions, whereas the background is obviously due to superimposed satellite transitions smeared out by charge and site disorder affecting both $\mathcal{H}_Q$ and $\mathcal{H}_\sigma$.

The temperature dependence of the ^{93}Nb central component spectra for pure SBN61 at $\angle(\vec{c}, \vec{B}_0) = 25°$ and $\vec{a} \perp \vec{B}_0$ is shown in Fig. 2. The line shapes of the Ce-doped SBN61 have a similar temperature dependence shifted for about 20 K to the lower temperatures. The width and position of the central component varies with temperature. The variation in the width is much smaller than the variation of the width of the ^{93}Nb central component in PMN,[6] where the central line is much narrower. In SBN the static EFG tensor (V_{ij}) distribution $P_S(V_{ij})$ induced by the substitutional charge disorder obviously dominates the site disorder induced by the glassy EFG distribution $P_G(V_{ij})$ reflecting dynamic polar nanoclusters. The distribution $P_G(V_{ij})$ is for each of the five EFG tensor elements an independent Gaussian distribution.[17]

The static substitutional disorder induced width of the NMR lines in SBN makes a determination of the local polarization distribution $W(p)$ from the NMR line shape rather difficult and unreliable. Thus one cannot make a straightforward discrimination between the SRBRF model and the RBRF Ising model on the basis of the difference between $W(p)$ in these two cases.

The temperature dependence of the ^{93}Nb effective spin-lattice relaxation time T_1 is presented in Fig. 3. On cooling from 450 K, T_1 slowly decreases with decreasing temperature down to 350 K and then starts to increase. The results show that we are similarly as in PMN (Ref. 6) in the fast motion regime $\Delta\omega\tau \ll 1$ above 250 K so that the analysis developed in Secs. III B and III C can be applied. The sharp increase in T_1 below T_c is the result of the development of long range order, i.e., the macroscopic polarization.

The temperature dependences of the first (M_1) and second (M_2) moments of the central component spectrum and the corresponding fits to the random-bond random-field Ising and SRBRF models (solid lines) are shown in Fig. 4 and Fig. 5, respectively.

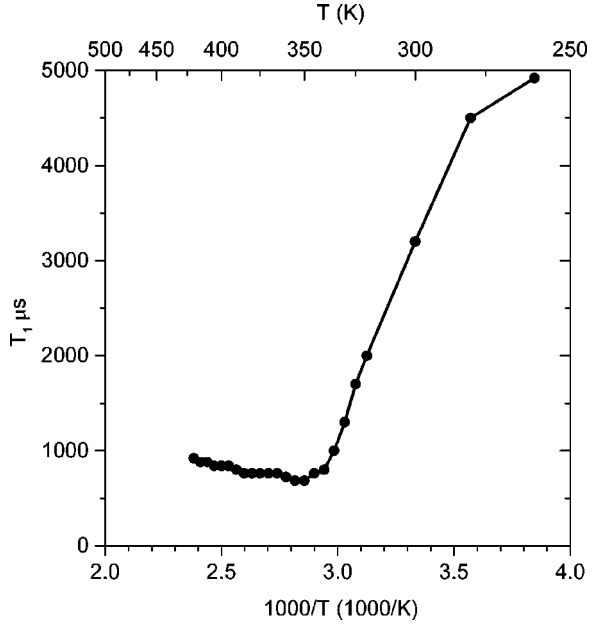

FIG. 3. Temperature dependence of ^{93}Nb spin-lattice relaxation time T_1 in SBN61 at $\nu = \nu_L + 200$ kHz. The solid line represents a guide for the eye.

In the Ising case (Fig. 4) the parameters in the expansion of the NMR frequency [Eq. (17)] are $\nu_0 = 2.8$ kHz, $\nu_1 = 7$ kHz, and $\nu_2 = -18$ kHz. The NMR spectrum is here obtained as

$$f(\nu) = \int_{-1}^{+1} \delta[\nu - \nu(p)] \frac{1}{2} [W(p) + W(-p)] dp \qquad (28)$$

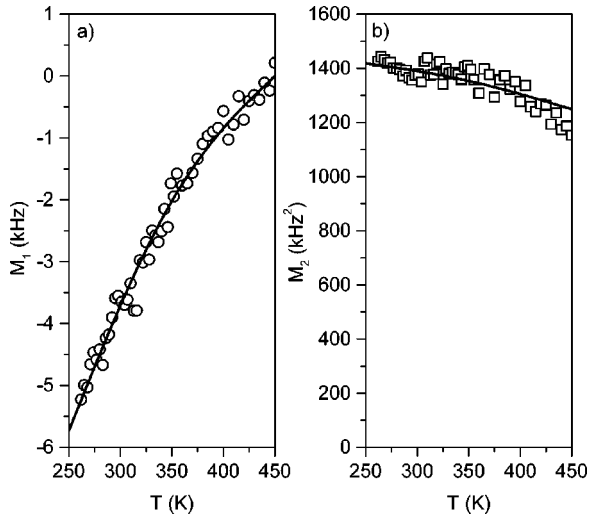

FIG. 4. Temperature dependence of (a) M_1 and (b) M_2 for the ^{93}Nb NMR line shape in SBN61 at $\theta = 25°$ The solid lines represent the corresponding fits from the RBRF Ising model with the parameters $J_0 = 485$ K, $J = 388$ K, and $\Delta/J^2 = 0.14$.

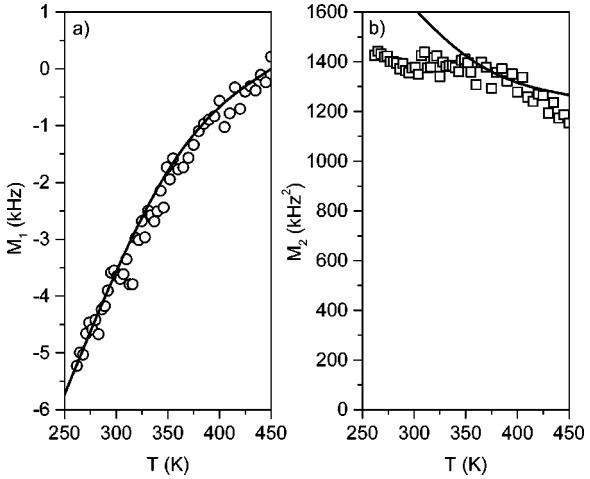

FIG. 5. The fits (solid lines) with the SRBRF model to the temperature dependences of the first M_1 (circles) and second M_2 (open squares) moments of the ^{93}Nb line shape. The SRBRF model parameters are $J_0=495$ K, $J=347$ K, and $\Delta/J^2=0.30$.

since two 180° domains with $+P$ and $-P$ exists in SBN for $T<T_c$. The first moment is here directly related to the glass order parameter q

$$M_1=\int_{-\infty}^{\infty}\nu f(\nu)\,d\nu=\nu_2 q, \tag{29}$$

whereas the second moment is more complex

$$M_2=\int_{-\infty}^{\infty}(\nu-\overline{\nu})^2 f(\nu)d\nu=\nu_1^2 q+\nu_2^2\int_{-1}^{+1}p^4 W(p)dp-\nu_2^2 q^2. \tag{30}$$

The RBRF Ising model parameters obtained from the fits are $J_0=485$ K, $J=388$ K, $\Delta=21210$ K^2, and $T_c=350$ K. It should be noted that the random field contribution $\Delta/J^2=0.14$ is here significantly larger than in PMN type relaxors, where $\Delta/J^2\approx 10^{-3}$.[6]

It should be stressed that the above set of parameters describes rather well the temperature dependences of both M_1 and M_2. Within the limits of experimental error it also describes the static linear susceptibility data obtained by Kleemann *et al.*[18] The M_2 data could not be well described with the SRBRF model as it can be seen from Fig. 5. Nevertheless it should be stressed that here too the random field contribution $\Delta/J^2=0.3$ turns out to be much larger than in perovskite type relaxors. The fact that the random field contribution in uniaxial SBN is much larger than in cubic relaxors is thus model independent.

The temperature dependence of the Edwards-Anderson glass order parameter obtained from the data in SBN61 according to the RBRF Ising model fit is shown in Fig. 6.

The inhomogeneous NMR linewidth as well as M_2 and M_1—and hence the glass order parameter q—are not much affected by the ferroelectric transition at T_c. This can be well understood in view of the huge random field contribution which smears out the glass transition.

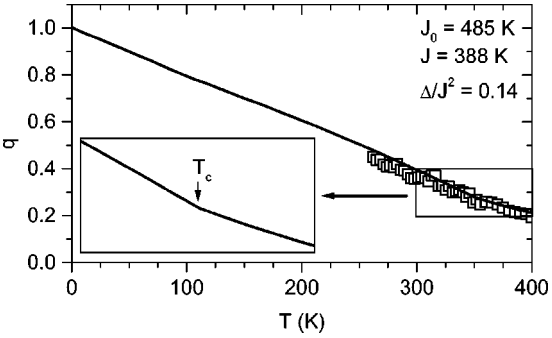

FIG. 6. Temperature dependence of the Edwards-Anderson glass order parameter q in SBN61, where the open squares represent the experimental values obtained from the ^{93}Nb NMR line shape and the solid line represents the fit to the RBRF Ising model with the parameters mentioned in the text. The change in the q vs T plot is shown in the inset.

To check on the onset of static long range order in SBN we decided to study the homogeneous linewidth, i.e., the temperature dependence of the effective spin-spin relaxation time T_2. In order to minimize the dynamic contribution, we decided to study the behavior at ν_L+200 kHz, i.e., the $T_{2\mathrm{eff}}$ of the satellite transitions where the $J(0)$ term is present as well.

As it can be seen in Fig. 7, T_2 is here practically T-independent between 450 K and 350 K. It should be noted that the homogeneous width given by $1/\pi T_2\approx 2$ kHz is much smaller than the inhomogeneous width 60 kHz of the spectrum (Fig. 2), thus confirming that the NMR spectra are in fact disorder induced inhomogeneous frequency distributions. Below $T_c=350$ K it sharply increases until a value of $T_2=950$ μs is reached. We believe that this limiting value is

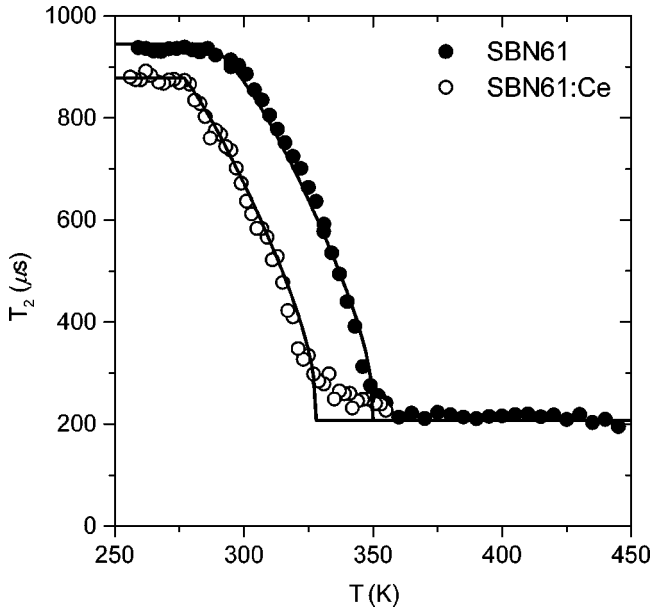

FIG. 7. Temperature dependence of ^{93}Nb spin-spin relaxation time T_2 in SBN61 and SBN61:Ce at $\nu=\nu_L+200$ kHz. The solid lines represent the fits with the Eqs. (32) and (33) and parameters $P_0=1.1$ and $\beta=0.15$.

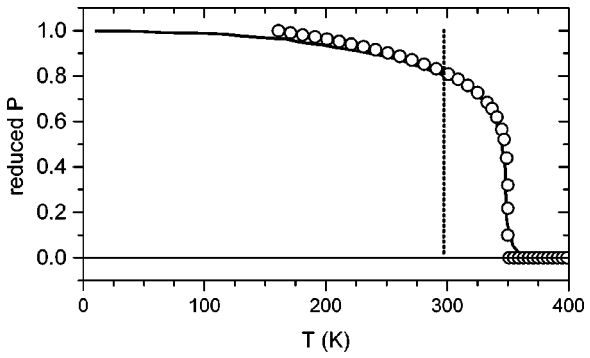

FIG. 8. Temperature dependence of the reduced polarization P in SBN61. The circles represent the polarization as determined from the NMR T_2 data, while the solid line represents the polarization as determined from the pyroelectric measurements of the polarization as determined by Glass *et al.* (Ref. 1). The critical exponent $\beta = 0.15$ was determined from the experimental points above the dotted line, i.e., close to T_c.

determined by the T-independent dipole-dipole contribution to the homogeneous linewidth. The critical quadrupolar contribution T_{2Q}^{-1} is now obtained from

$$\frac{1}{T_{2\text{eff}}} = \frac{1}{T_{2Q}} + \frac{1}{T_{2D-D}}, \tag{31}$$

where $T_{2D-D} = 950\ \mu$s.

The T-dependence of T_{2Q} given by

$$\frac{1}{T_{2Q}} \propto (1-P^2)^{(3/2)} \tag{32}$$

can be now well described with the T dependence of the spontaneous polarization (Fig. 8)

$$P = P_0 \left(\frac{T_c - T}{T_c} \right)^{\beta}, \tag{33}$$

where the exponent $\beta = 0.15 \pm 0.03$ is within the limits of the experimental error the same as the one obtained by Glass[1] in the pyroelectric measurement of the spontaneous polarization (Fig. 7) in SBN60. Here $P_0 = 1.1$.

A fit which is not quite as good can be obtained by the $D=3$ Ising model critical exponent $\beta = 0.31$ but not with the spherical model exponent $\beta = 0.5$. It should be mentioned that the obtained rather low value of the order parameter exponent $\beta = 0.15 \pm 0.03$ is compatible with the numerical estimates for the $D=3$ random field Ising model $\beta = 0.06 \pm 0.07$.[19] It should be also noted that the critical exponent $\beta = 0.35$ of the dilute(d) Ising model,[20] which belongs to the same universality class as the random exchange model, is significantly higher than the experimental value in SBN.

In fact in SBN both random fields and random bonds are present, as shown by the M_1 and M_2 results. In the presence of both random fields and random bonds, one of these two contributions becomes dominant and suppresses the effect of the other as far as the value of the effective critical exponent is concerned.[21] The above results thus seem to show that in SBN the order parameter critical exponent β is dominated by random fields rather than by random bonds.

This finding corroborates previous inferences when discussing tendencies of other critical exponents deduced from linear birefringence data, $\nu \rightarrow 1$ and $\gamma \rightarrow 1.8$,[8] in accordance with predictions of the three-dimensional random-field Ising model.[19]

In connection with the description of the T_2 data in terms of critical exponents it should be noted that there is no discontinuity in the NMR T_2 data nor in the slowly cooled susceptibility data, which would give hint at a possible first-order phase transition in SBN and SBN:Ce. One should also mention that in order to be sure, the linear birefringence has been carefully measured as a function of temperature at cooling rates 10 mK/min in order to avoid any smearing effects due to the expected large critical slowing down. The measurements have been done on microscopically small regions of the sample ($\approx 20 \times 20 \times 100\ \mu\text{m}^3$), hence avoiding temperature gradients.

V. CONCLUSIONS

The ^{93}Nb NMR spectra of the uniaxial relaxor compounds SBN61 and SBN61:Ce are dominated by substitutional charge disorder rather than by site disorder. Nevertheless a careful analysis of the data allowed for a determination of the random-bond and random-field contributions as well as for a determination of the temperature dependence of the Edwards-Anderson glass order parameter. The random-field contribution is in SBN by two orders of magnitude larger than in cubic relaxors like PMN where the order parameter is quasicontinuous. The polar order parameter P as measured by the spin-spin relaxation time T_2 steeply increases below T_c with a critical exponent which within the limits of experimental error agrees with $D=3$ random field Ising model one. Though both random bonds and random fields are present, the critical behavior close to T_c is dominated by random fields and is of the 3D-random field Ising model type.

ACKNOWLEDGMENTS

The authors would like to thank the Ministry of Education, Science and Sport of Slovenia, the German Bundesministerium für Bildung und Forschung, and Deutsche Forschungsgemeinschaft for financial support, and Dr. B. Tadić for useful discussions on the random field critical exponents.

APPENDIX A: COEFFICIENTS C_0, C_1, AND C_2

The coefficients C_0, C_1, and C_2 determining the dependence of the spin-spin relaxation rate T_2^{-1}

$$T_2^{-1} = C_0 \left| \frac{eQ}{h} \right|^2 J(0) + C_1 \left| \frac{eQ}{h} \right|^2 J(\omega_L) + C_2 \left| \frac{eQ}{h} \right|^2 J(2\omega_L) \tag{A1}$$

on the spectral densities $J(0)$, $J(\omega_L)$, and $J(2\omega_L)$ are shown in Table I for some typical values of the nuclear spin I.

TABLE I. Coefficients C_0, C_1, and C_2 for different nuclear spin I values as determined from Eqs. (6a)–(6c). The transitions $m \leftrightarrow m+1$ labeled with positive numbers m are omitted, since symmetric satellite transitions ($m \leftrightarrow m+1$ and $-m \leftrightarrow -m+1$) have the same spin-spin relaxation rate T_2^{-1}.

I	$m \leftrightarrow m+1$	C_0	C_1	C_2
1	$-1 \leftrightarrow 1$	22.21	14.80	9.87
3/2	$-3/2 \leftrightarrow -1/2$	9.87	6.58	6.58
3/2	$-1/2 \leftrightarrow +1/2$	0	6.58	6.58
2	$-2 \leftrightarrow -1$	5.55	5.35	4.11
2	$-1 \leftrightarrow 0$	0.62	3.70	5.76
5/2	$-5/2 \leftrightarrow -3/2$	3.55	4.74	2.76
5/2	$-3/2 \leftrightarrow -1/2$	0.98	3.55	4.54
5/2	$-1/2 \leftrightarrow +1/2$	0	1.58	5.53
3	$-3 \leftrightarrow -2$	2.47	4.28	1.97
3	$-2 \leftrightarrow -1$	0.89	3.75	3.55
3	$-1 \leftrightarrow 0$	0.10	1.38	4.87
7/2	$-7/2 \leftrightarrow -5/2$	1.81	3.89	1.48
7/2	$-5/2 \leftrightarrow -3/2$	0.81	3.89	2.82
7/2	$-3/2 \leftrightarrow -1/2$	0.20	1.75	4.16
7/2	$-1/2 \leftrightarrow +1/2$	0	0.67	4.70
9/2	$-9/2 \leftrightarrow -7/2$	1.10	3.29	0.92
9/2	$-7/2 \leftrightarrow -5/2$	0.62	3.93	1.87
9/2	$-5/2 \leftrightarrow -3/2$	0.27	2.56	3.02
9/2	$-3/2 \leftrightarrow -1/2$	0.07	1.01	3.88
9/2	$-1/2 \leftrightarrow +1/2$	0	0.37	4.20

APPENDIX B: SPECTRAL DENSITY OF THE EFG AUTOCORRELATION FUNCTION IN AN ASYMMETRIC DOUBLE POTENTIAL WELL

A particle moving in an asymmetric double potential well can be described with the probabilities of finding the particle in a given potential well. These obey the master equations

$$\dot{n}_- = -n_- W_{-+} + n_+ W_{+-}, \tag{B1a}$$

$$\dot{n}_+ = -n_+ W_{+-} + n_- W_{-+}, \tag{B1b}$$

where n_- and n_+ are the probabilities of finding the particle in the higher (with a dipole moment -1) and lower (with a dipole moment $+1$) local minimum, respectively. W_{-+} and W_{+-} are the probabilities per unit time of a transition from a higher to a lower minimum and vice versa. These two probabilities per unit time are assumed to be thermally activated and can be expressed in the following form:

$$W_{-+} = W_0 \exp\left(+\frac{1}{2}\frac{\Delta E_p}{kT}\right), \tag{B2a}$$

$$W_{+-} = W_0 \exp\left(-\frac{1}{2}\frac{\Delta E_p}{kT}\right), \tag{B2b}$$

$$W_0 = \tau_\infty^{-1} \exp\left(-\frac{\Delta E_0}{kT}\right). \tag{B2c}$$

Here ΔE_0 is the height of the potential barrier and τ_∞ the correlation time in the absence of the polarization at very high temperatures. The asymmetry ΔE_p is the difference between the height of the potentials of the higher and lower minimum of the asymmetric double potential well. It is related to the polarization p as

$$p = \tanh\left(\frac{\Delta E_p}{2kT}\right). \tag{B3}$$

By introducing a new variable $\Delta p = (n_+ - n_-) - p$ and noting that $n_+ + n_- = 1$ the master equations, Eq. (B1a), have a particularly simple solution:

$$\Delta p(t) = \Delta p(t=0) \exp\left(-\frac{t}{\tau}\right), \tag{B4}$$

where

$$\tau = (W_{-+} + W_{+-})^{-1} = \tau_\infty \exp\left(\frac{\Delta E_0}{kT}\right)\sqrt{1-p^2}. \tag{B5}$$

The autocorrelation function is then

$$\Delta p(0)\Delta p(t) = \Delta p(0)^2 \exp\left(-\frac{t}{\tau}\right). \tag{B6}$$

The average autocorrelation function $\overline{\Delta p(0)\Delta p(t)}$ is then found as the thermal average of two cases, i.e., for the particle in the higher $\Delta p(0) = -1 - p$ and in the lower $\Delta p(0) = 1 - p$ potential well minimum

$$\overline{\Delta p(0)\Delta p(t)} = \frac{\exp(\Delta E_p/2kT)(1-p)^2 + \exp(-\Delta E_p/2kT)(1+p)^2}{Z} \exp\left(-\frac{t}{\tau}\right), \tag{B7}$$

where $Z = \exp(\Delta E_p/2kT) + \exp(-\Delta E_p/2kT)$. The real part of the spectral density $J(\omega)$ is finally

$$J(\omega) = \int_0^\infty \overline{\Delta p(0)\Delta p(t)} \exp(-i\omega t)\, dt = (1-p^2)\frac{\tau}{1+\omega^2\tau^2}, \tag{B8}$$

with τ given by expression (B5).

[1] A.M. Glass, J. Appl. Phys. **40**, 4699 (1969).
[2] G.A. Smolenskii and V.A. Isupov, Dokl. Akad. Nauk SSSR **97**, 653 (1954).
[3] L.E. Cross, Ferroelectrics **76**, 241 (1987).
[4] P.B. Jamieson, S.C. Abrahams, and J.L. Bernstein, J. Chem. Phys. **48**, 5048 (1968).
[5] W. Kleemann, J. Dec, P. Lehnen, T. Woike, and R. Pankrath, in *Fundamental Physics of Ferroelectrics 2000*, edited by R. E. Cohen (American Institute of Physics, New York, 2000), Vol. CP535, p. 26.
[6] R. Blinc, J. Dolinšek, A. Gregorovič, B. Zalar, C. Filipič, Z. Kutnjak, A. Levstik, and R. Pirc, Phys. Rev. Lett. **83**, 424 (1999).
[7] R. Blinc, B. Zalar, A. Gregorovič, R. Pirc, V.V. Laguta, and M.D. Glinchuk, Phys. Rev. B **63**, 024104 (2001).
[8] P. Lehnen, W. Kleemann, T. Woike, and R. Pankrath, Eur. Phys. J. B **14**, 633 (2000).
[9] R. Pirc and R. Blinc, Phys. Rev. B **60**, 13 470 (1999).
[10] R. Blinc, A. Gregorovič, B. Zalar, R. Pirc, and S.G. Lushnikov, Phys. Rev. B **61**, 253 (2000).
[11] R. Blinc, A. Gregorovič, B. Zalar, R. Pirc, V. Laguta, and M. Glinchuk, J. Appl. Phys. **89**, 1349 (2001).
[12] R. Blinc, J. Dolinšek, R. Pirc, B. Tadić, B. Zalar, R. Kind, and O. Liechti, Phys. Rev. Lett. **63**, 2248 (1989).
[13] W. Kleemann, V. Bobnar, J. Dec, P. Lehnen, R. Pankrath, and S. A. Prosandeev, Ferroelectrics (to be published).
[14] J. Dec, W. Kleemann, T. Woike, and R. Pankrath, Eur. Phys. J. B **14**, 627 (2000).
[15] A. Abragam, *The Principles of Nuclear Magnetism* (Oxford University Press, London, 1961).
[16] R. Pirc, B. Tadić, and R. Blinc, Phys. Rev. B **36**, 8607 (1987).
[17] R. Kind, R. Blinc, and M. Koren, Phys. Rev. B **37**, 4864 (1988).
[18] J. Dec, W. Kleemann, V. Bobnar, Z. Kutnjak, A. Levstik, R. Pirc, and R. Pankrath (unpublished).
[19] M.E. Newman and G.T. Barkema, Phys. Rev. E **53**, 393 (1996).
[20] H.G. Ballesteros, L.A. Fernández, V. Martin-Mayor, A. Muñoz Sudupe, G. Parisi, and J.J. Ruiz-Lorenzo, Phys. Rev. B **58**, 2740 (1998).
[21] B. Tadić (private communication).